Journal of Micromechanics and Microengineering

PAPER • OPEN ACCESS

Passive communication for low power distributed sensors using MEMS optical cavities

To cite this article: Jacob Schopp and Shamus McNamara 2024 *J. Micromech. Microeng.* **34** 035011

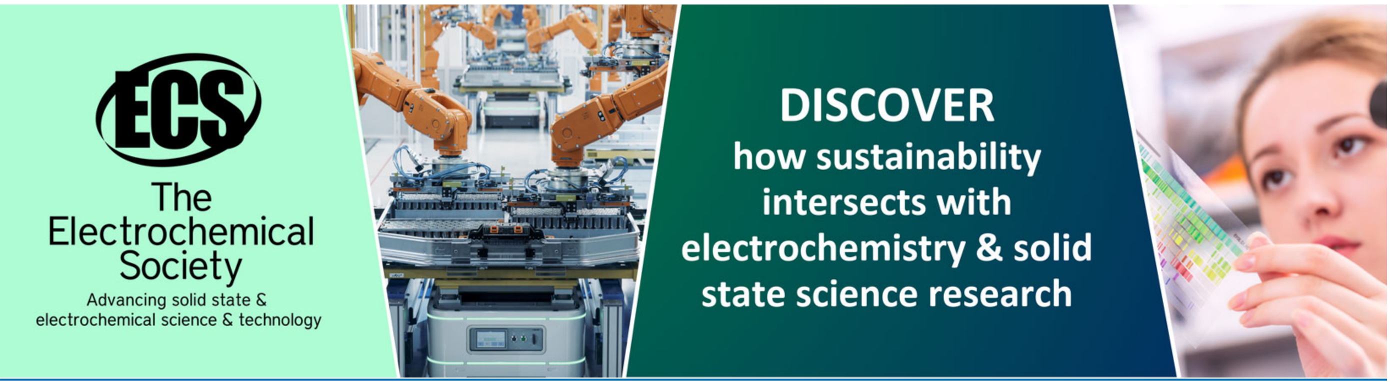

OPEN ACCESS
IOP Publishing

Journal of Micromechanics and Microengineering

J. Micromech. Microeng. **34** (2024) 035011 (8pp)

https://doi.org/10.1088/1361-6439/ad2910

Passive communication for low power distributed sensors using MEMS optical cavities

Jacob Schopp* and **Shamus McNamara**

Department of Electrical and Computer Engineering, University of Louisville, Louisville, KY, United States of America

E-mail: schoppjacob@gmail.com

Received 6 November 2023, revised 18 January 2024
Accepted for publication 13 February 2024
Published 23 February 2024

Abstract

Distributed sensing has been of great interest in recent research. Distributed sensors are in part defined by the methods they use to communicate. We demonstrate a new low power method of optical communication. Instead of communicating optically by generating new light to communicate using a light emitting diode or laser, our method uses optical interference to vary the reflectivity of a micro-electromechanical systems (MEMS) optical cavity. A thin air gap between an adjustable MEMS mirror made on a silicon on insulator die and glass encapsulation generates optical interference. By moving the mirror electrostatically, the reflected light intensity is modulated, and signals are transmitted passively. The transmitted signal is measured by observing the reflected light intensity with a photodiode. We demonstrate the use of fiber optic cables to deliver illumination and collect reflected light with modulated intensity. We propose that these devices may also be used in series arrays where reflected light from one optical cavity can be used as illumination for another.

Keywords: MEMS, optical communication, low power, optical interference, electrostatic actuation, optical fiber

1. Introduction

Distributed sensing has been the subject of much interest and recent research, acting as an enabling technology for growth in new fields such as robotic touch sensing [1, 2], shape sensing [3], temperature sensing [4], structural health monitoring [5, 6], and more. Continued development of distributed sensing methods will enable new technologies which are not currently possible.

Further improvements in distributed sensors will require increasing sensor density and reducing sensor size, power consumption, and interconnection complexity. We present a novel method of sensor interconnection that addresses these demands using micro-electromechanical systems (MEMS) optical cavities to perform low power passive communication over optical fibers. Distributed sensors can be categorized by the methods in which they are connected to themselves and to the outside world. Distributed sensors can be broadly split into three groups: those which are connected using wired connections, wireless connections, and optical connections.

Wired sensors are common, they can have a wide range of sensor options and leverage existing electronics technology. Wired distributed sensors, however, can have bulky bundles of wires that limit the number of sensors that may be utilized, and they can be difficult to manufacture due to the large number of interconnections.

* Author to whom any correspondence should be addressed.

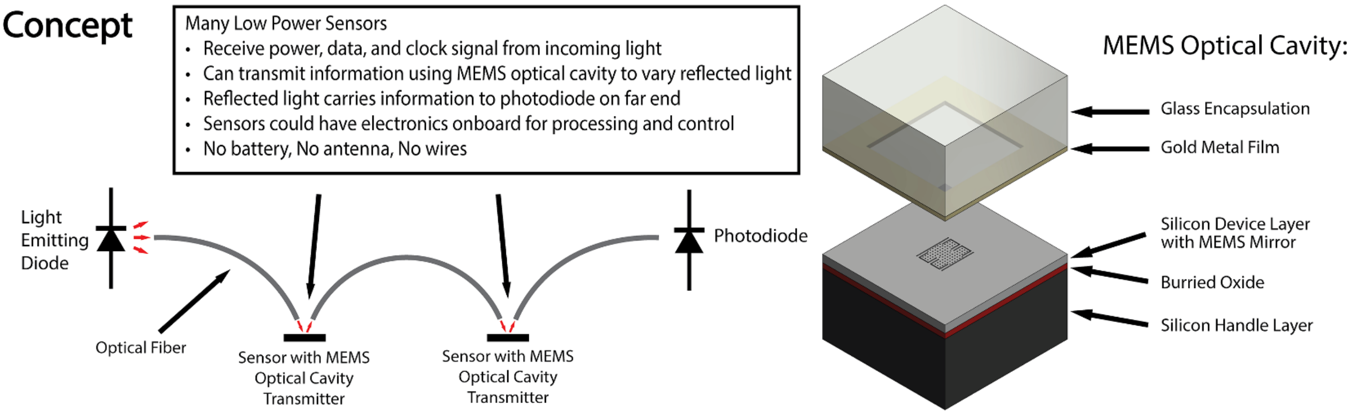

Figure 1. Method of communication using passive MEMS reflection.

Wireless sensors resolve some of the issues of wired connections. They offer portability, physically simple interconnection, and remove the constraints of being physically tethered to a wire. They are popular in a number of sensing applications but come with several drawbacks [7]. Wireless sensors need power which must be delivered, collected, or stored in some way [8, 9]. This is resolved by an increase in either size or complexity. Shrinking of antennas and batteries is difficult, placing limitations on further reduction of the size of wirelessly connected devices.

Optically connected sensors can resolve some of these issues. Like wireless radio frequency (RF) methods, light can be used for power and data delivery. Optical sensing methods, especially fiber-based methods, are used in many applications including strain and vibration sensing [10], temperature sensing [4], and chemical and biological sensing [11, 12]. Two main methods of fiber-based sensing prevail: fiber Bragg grating sensors which rely on the deformation of optical gratings [13, 14], and optical time domain reflectometry [15, 16], which relies on the back-scattering of light using Rayleigh, Ramen, and Brillouin effects. Fiber-based methods however, usually require an external fiber interrogator to perform measurements and the sensing capabilities are limited by the optical phenomena they observe. The measurements they take are from locations distributed along the fiber but the measurement electronics are centralized.

We propose to attach MEMS devices along an optical fiber without the use of electrical wires. The incoming light provides power and may be modulated to provide communication to the MEMS sensor, as illustrated in figure 1. The benefits include simplicity, no batteries, and no wires. The drawback of this method is that the only power available to the MEMS sensor is the optical power, and most of the light must be transmitted to the next sensor if many sensors are to be utilized. This limits the power available to the μW range. This necessitates a very low power method of sending data from the MEMS sensor.

In this work, we propose to address the communication problem by utilizing a MEMS optical cavity for low power, passive communication. The light incident on the MEMS device reflects off the optical cavity whose reflectivity can

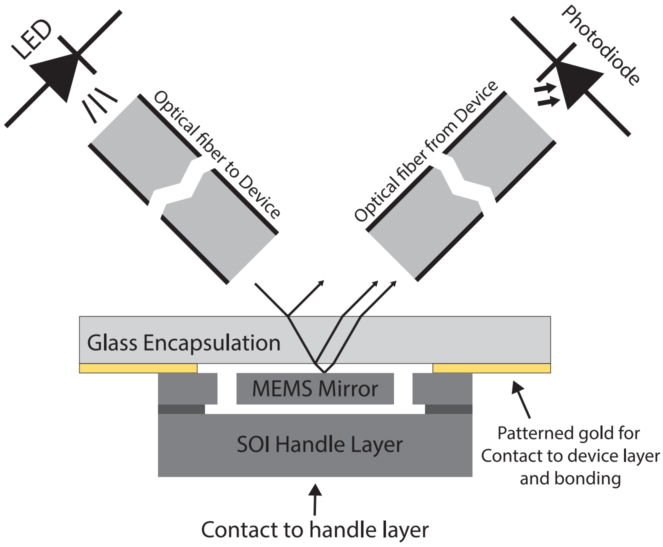

Figure 2. Schematic of MEMS optical cavity.

be modulated using electrostatic actuation. In this paper, a very low power communication method is demonstrated. Additionally, this method is very small as the MEMS mirror measures only 200 μm by 250 μm. This size is smaller than antennas used for RF communications.

2. System design

This paper focuses on reducing the size, weight, power consumption, and connection complexity of distributed sensors with a new communication method using passively reflecting, exceptionally low power, electrostatically actuated MEMS optical cavities. We demonstrate communication with energy per bit on the tens of picojoule scale, size on the hundreds of micrometer scale, and straightforward sensor interconnection. This method can be used with onboard digital electronics, low power electrically connected sensors, and without batteries or bulky bundles of wires.

Our proposed method is shown in figures 1 and 2. In this method monochromatic light is sent into an optical fiber on one side using an light emitting diode (LED). This light is, in part, used for power by sensors which are coupled to the fiber. The devices may use this power internally to perform sensing with a low power electrically connected sensor. This power can also be used for onboard electronics to manage the processing and transmission of information. Once information is gathered the sensors can transmit their collected data. Rather than creating new light using an LED or other light source, the sensors instead transmit their data by modulating the reflectivity seen by light in the fiber. Reflectivity can be modulated using an optical cavity whose dimensions can be changed by moving an electrostatically actuated MEMS mirror. The reflected light with modulated intensity is coupled back into an optical fiber where it continues either to another device or to a photodiode receiver. We envision sensors could be arrayed in series or parallel with one or more fibers connecting to multiple sensors. The reflected light transmission can be received using a photodiode attached to the far side of the optical fiber.

The incident light can also be modulated to send signals to the connected sensors. The illumination can have a constant and varied component. The constant illumination provides power and light for reflection. The varied component can be used to send data and a clock signal.

The fiber and the device could be coupled in several ways. As shown in figure 1 and demonstrated later in this paper, the fiber can be discontinuous where one fiber delivers light and the other collects the reflected light. It may also be possible to notch the fiber so that a small portion of the light leaves, reflects off the sensor, and returns into the fiber. In an ideal coupling between the optical fiber and the optical cavity, most of the illumination light should be delivered to the MEMS optical cavity and most of the reflected light from the optical cavity should be routed to the photodiode receiver. There are many unexplored coupling options. This is an area of ongoing research.

3. Design

We fabricated a MEMS optical cavity which demonstrates communication using passive optical interference. Because we only seek to demonstrate communication with a MEMS optical cavity, the fabricated device does not require onboard electronics, photovoltaics for power collection, or other features. This proof-of-concept device is powered externally for simplicity.

As shown in figure 2, the MEMS optical cavity consists of two parts, a movable MEMS mirror and glass encapsulation. The two are closely spaced with a thin air gap in between. This resembles a Fabry–Pérot interferometer whose cavity gap can be varied electrostatically. When the mirror is moved, the size of the air gap is varied so that more or less of the incoming light will constructively or destructively interfere and the reflected light intensity will change.

The sprung mirror shown in figure 3 measures 200 μm by 250 μm. For ease of handling, the MEMS die is 3.3 mm by 3.3 mm and the glass encapsulation die is 5.95 mm by 5.95 mm. The glass die is larger than the MEMS die so that electrical contact can be conveniently made from the backside to the MEMS mirror on the device layer via the metal film on the glass. In application the device could be made considerably smaller.

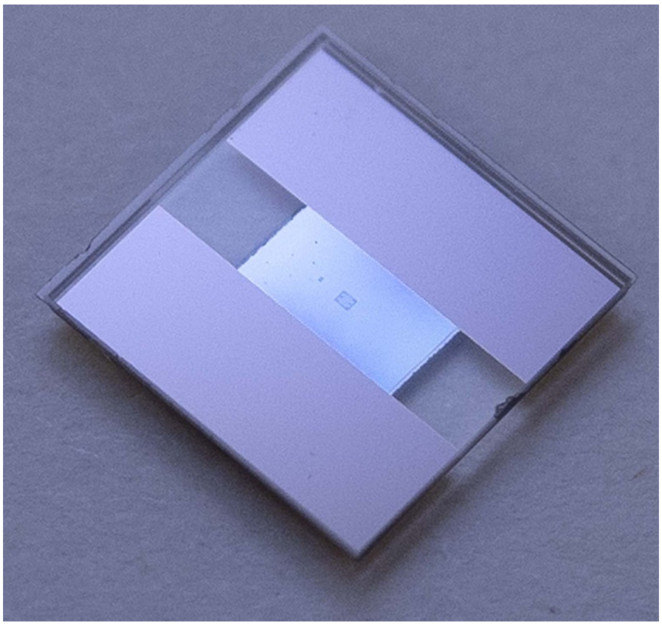

Figure 3. Assembled device with SOI MEMS die and glass encapsulation. MEMS mirror is visible through the glass in the center of the SOI die.

The MEMS mirror and the springs that support it are created from the silicon device layer of a silicon on insulator (SOI) wafer. SOI wafers are an excellent starting point for the construction of these MEMS optical cavities because they can be purchased with precise device layer and buried oxide layer thicknesses. Electrostatic force between the handle layer and the device layer moves the MEMS mirror towards the substrate, increasing the thin air gap between the surface of the mirror and the glass encapsulation. It is by this mechanical movement that the reflectivity of the device is varied to transmit data.

The MEMS mirror must have springs with appropriate stiffness for a frequency response high enough to send data at reasonable speed and strength to withstand shock during fabrication and use. The springs and mirror were designed and simulated in CoventorWare. CoventorWare is a common tool for the mechanical and electrostatic simulation of MEMS devices. The best design is shown in figure 4 and is used in all other figures. This design was the most successful, proving to be robust during fabrication and having a convenient 35 V maximum safe electrostatic actuation voltage. The simulated spring constant was estimated to be 26 475 μN μm^{-1}. The device layer is 12 μm thick, and the sprung mass is approximately 1.1 μg. Using the sprung mass and spring constant, the natural frequency can be calculated to be about 780 kHz. However, the CoventorWare simulation shows that the design will be overdamped due to squeeze-film effects when the small

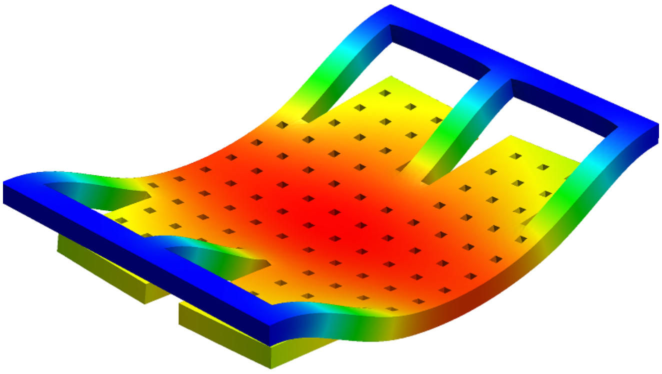

Figure 4. CoventorWare simulation of MEMS mirror when actuated. Deflection is exaggerated.

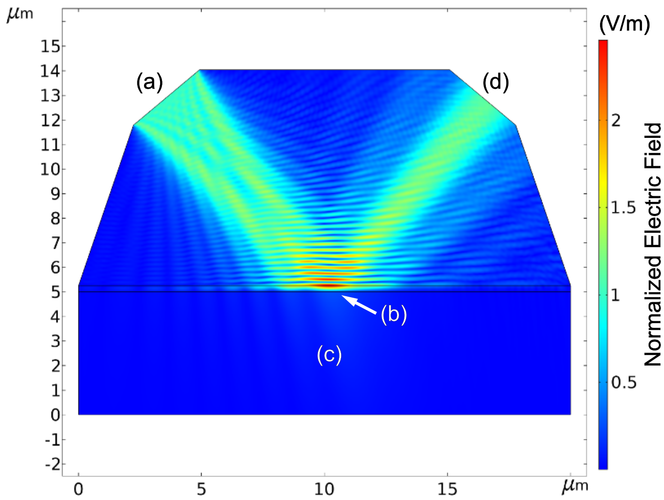

Figure 5. COMSOL wave optics electromagnetic frequency domain simulation of reflection. Light enters at glass boundary at top left (a), interacts with optical cavity formed by air gap (b) and truncated silicon mirror surface (c), and reflected light leaves at top right (d).

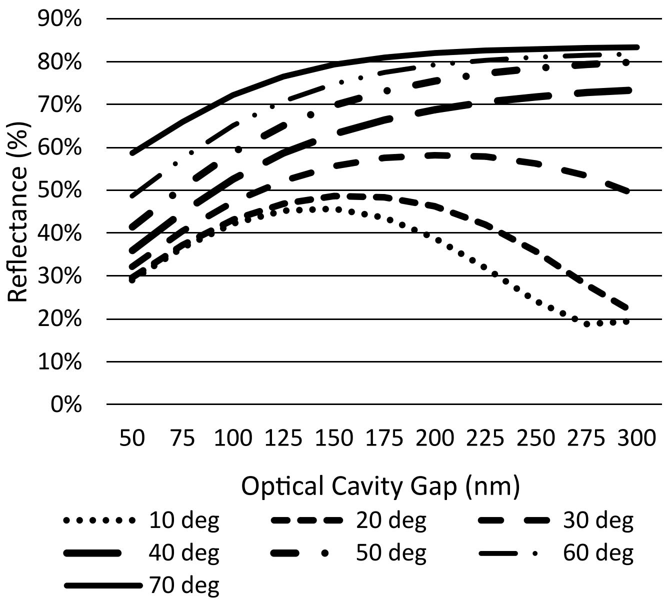

Figure 6. COMSOL simulation results showing relationship between optical cavity gap, angle, and reflectance.

optical gap is considered, and the squeeze-film effects add a frequency dependent spring constant. The mirror is perforated with ninety-four 5 μm by 5 μm square holes spaced 20 μms center to center, The perforations were added to aid with the anhydrous vapor HF release of the mirror. The mirror is sprung using cantilever springs which are sized so that the mirror moves down while remaining reasonably flat. If the springs are too short, or too long, the mirror will bend into a 'U' shape that either droops in the middle or on the tips. The surface of the mirror has an area of 39 200 μm^2 subtracting perforations.

The range of movement of the MEMS mirror is determined by the thickness of the buried oxide that the mirror actuates across. Due to the use of electrostatic actuation, the buried oxide must be at least three times greater in thickness than the maximum displacement of the mirror to avoid pull-in. In this design, a buried oxide thickness of 500 nm was selected. This means that the maximum possible actuation before pull-in is roughly 166 nm. This is more than is required.

COMSOL Wave Optics was used to perform electromagnetic waves frequency domain simulations to determine the relationship between the optical cavity gap, the angle of the incident light, and the resulting reflectance. The simulation shown in figure 5 represents a small portion of the optical cavity that is 20 μm wide. Light with a 550 nm wavelength is sent in from the top left through the glass towards the optical cavity in the middle. Using COMSOL's scattering boundary condition, all boundaries were made to be transparent. The scattering boundary condition at the top left was modified to include a 1 V m^{-1} amplitude wave traveling inwards, with the incident wave propagating perpendicular to the surface. The reflected light exits on the top right boundary. On the bottom is a truncated portion of the silicon device layer. The thin air gap is between the upper glass portion and the lower silicon portion. COMSOL's default material properties were used. The type of glass used is called 'Glass (quartz).' The indices of refraction are 1.5, 1, and 4.07 for the glass, air, and silicon respectively, with the silicon having an optical extinction coefficient of 0.03.

The air gap thickness and the incident angle are both varied in simulation to determine their relationship with reflectance. The results are shown in figure 6. Reflectance here is taken as the ratio between the optical power exiting through the top right boundary to the power entering through the top left boundary. The angle of incidence is taken here as the angle from normal to the surface of the mirror.

From the simulation results it can be seen that at very small optical cavity gaps between 50 nm and 150 nm the reflectance at all simulated angles increases with the optical cavity gap size. This is promising for modulating the reflectance of light from a wide range of incident angles, but such a small gap was avoided because of the risk that a collision between the MEMS mirror and the glass encapsulation would result in stiction. We instead aimed to operate the device with a larger optical cavity gap, where the reflectance at large (glancing) angles of incidence are fairly consistent, while at low (normal) angles of incidence the reflectance varies greatly with cavity

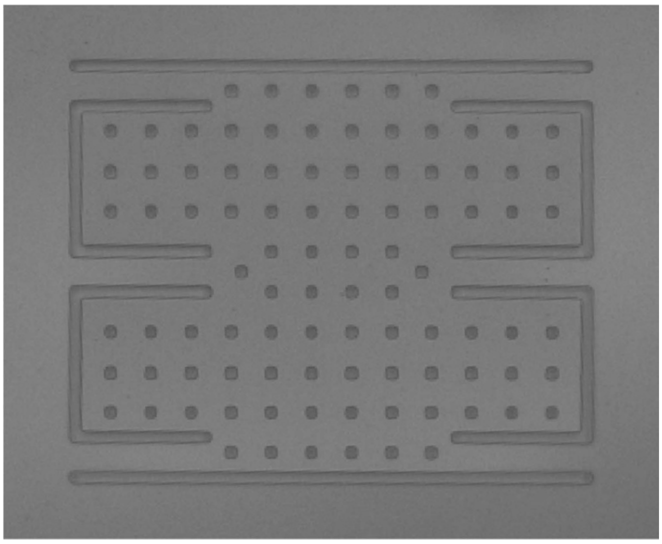

Figure 7. Micrograph of MEMS mirror.

gap. We identified the region between 200 nm and 250 nm to be the intended operating range.

The mirror and the glass encapsulation are initially spaced apart by a small distance to avoid stiction and to minimize the distance that the mirror is required to travel. To actuate in the identified area between 200 nm and 250 nm, an initial optical gap was chosen to be slightly less than the lower bound, at 175 nm. This distance is physically set by the metal film on the glass encapsulation. The mirror can move up to 166 nm, one third the distance between the bottom of the device layer and the top of the handle layer. Because the initial optical gap is 175 nm, the optical cavity can be larger than 300 nm without pull-in, which is more than the 250 nm desired

4. Fabrication

Figure 7 shows an image of the fabricated MEMS mirror taken with a Zygo NewView 7300 optical profilometer. The figure shows the 'H' shaped perforated mirror, supported by six cantilever springs. The image has been rotated, cropped, and its format changed but has been otherwise unmodified.

The MEMS mirror is fabricated using the process shown in figure 8. The MEMS mirror is made on an SOI substrate with a 12 $\pm$ 1 μm device layer and a 0.5 μm $\pm$ 5% buried oxide. The device layer is patterned and etched using photolithography and deep reactive ion etching (DRIE). After etching, and before release, the wafer is diced, and the die are cleaned. The MEMS mirrors are then released using anhydrous-HF etching.

The glass encapsulation is made from a 500 μm thick SCHOTT Borofloat 33 glass substrate. This substrate was selected for it is flatness and optical clarity. The metal which determines the initial optical cavity gap is sputtered onto the glass substrate. The metal is 20 nm of titanium adhesion layer followed by 155 nm of gold. Together this results in the 175 nm intended initial optical cavity gap.

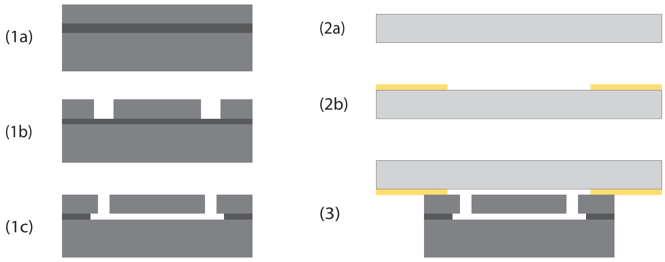

Figure 8. Fabrication process. (1a) MEMS process begins on SOI wafer. (1b) DRIE etching followed by dicing and cleaning. (1c) Vapor HF release. (2a) Encapsulation die begins on glass substrate. (2b) Gold is sputtered and patterned followed by dicing. (3) MEMS die and glass encapsulation die are attached.

After fabrication of the MEMS SOI die it is attached to the glass encapsulation die. The thickness of the gold deposited on the glass die controls the distance between the glass and the MEMS die. The die can be easily assembled by pressing their surfaces together and gluing at the perimeter with UV cured adhesive. Thermocompression bonding may be an excellent alternative to adhesive as it has been demonstrated to be possible with very thin bond frames, which may allow for a small device footprint [17, 18].

5. Evaluation

The mirror's displacement over a range of applied voltages was determined by inspecting a die without glass encapsulation using an optical profilometer. The top row of figure 9 shows the measured displacement of the mirror as voltage is varied between 0 V and 35 V. As the voltage is increased, the mirror deflects downward into the substrate and moves up to 100 nm at 35 V. Further voltages were not tested due to the risk of pull-in.

As shown in figure 10, the relationship between applied voltage and deflection can be used to estimate the spring constant. We estimate the spring constant to be about 58% of the simulated spring constant, at 15 359 μN μm^{-1}. Overetching of the springs, manufacturing tolerance on the SOI wafer device layer thickness, and stresses within the device layer are likely contributing factors. The MEMS optical cavity works as intended, but requires reduced actuation voltages.

The device used in the lower half of figures 9–11 has a minor defect where the device did not completely release in one corner but still functions well.

The optical interference effect is visible through a typical microscope with white light illumination. When a voltage is applied, the deflection of the springs widens the gap between the glass encapsulation and the mirror resulting in a color change visible in the microscope. As seen in the lower row of figure 9, the die changes from blue to yellow in appearance as the voltage is increased from 0 V to 35 V.

To observe change in reflectivity, a constant red laser light was shined onto the device's surface and the reflected light was sent to a photodiode. When the MEMS optical cavity is

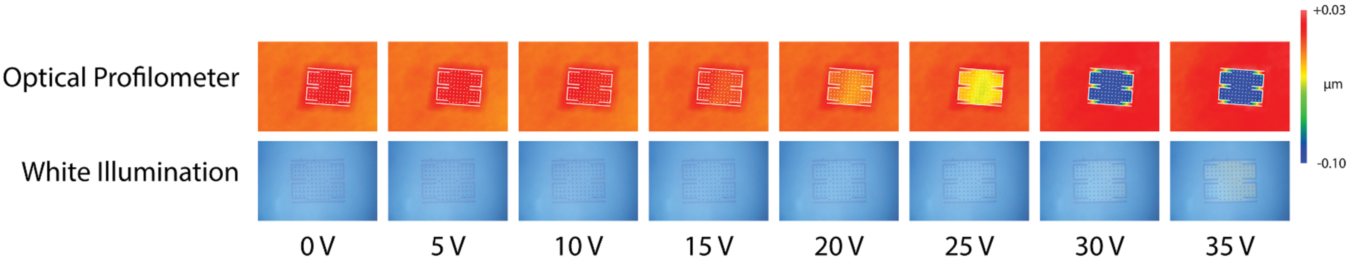

Figure 9. Change in optical profilometer (top) and visible color in microscope (bottom) due to electrostatic deflection.

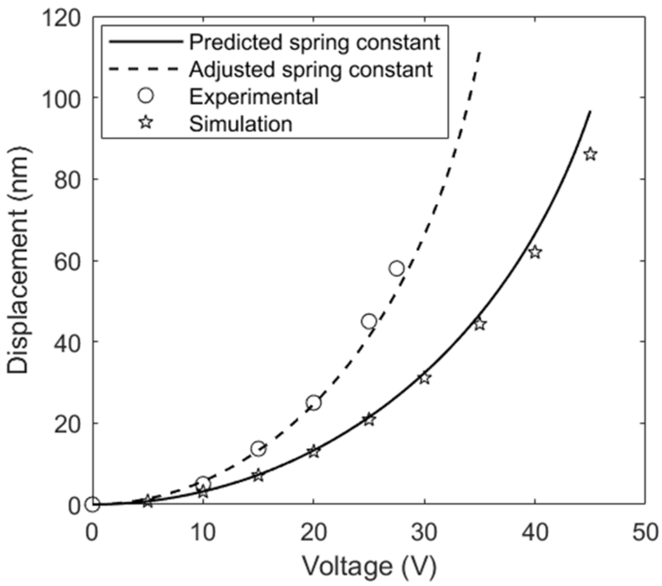

Figure 10. Displacement of the MEMS mirror over a range of voltages including simulation (stars) and experimental data (circles). Curves using the predicted (solid) and adjusted (dashed) spring constants are also shown.

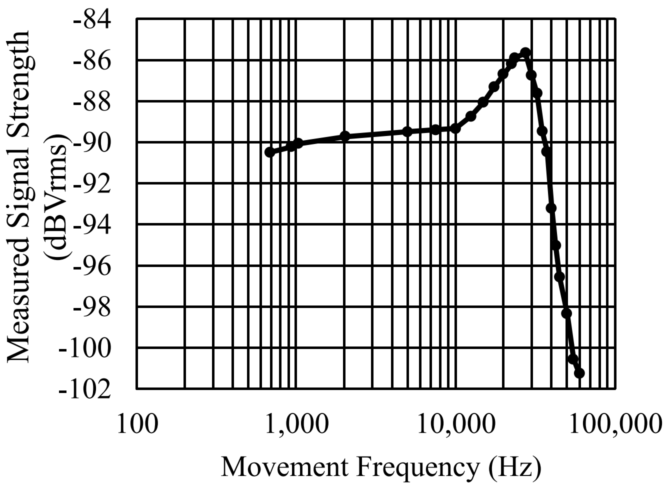

Figure 11. Frequency response of the device as measured using laser reflection into a photodiode.

actuated, a change in the reflected light intensity is detected at the photodiode. A function generator was used to actuate the MEMS optical cavity with a 10 V_{peak} sine wave at a frequency of 195 Hz. The generated sine wave is centered around zero volts. The MEMS optical cavity is actuated twice every period of the sine wave because the deflection is electrostatic, and the force is attractive during both the negative and positive half cycle, doubling the frequency of the reflected light intensity. The photodiodes signal was first amplified using a Stanford Research Systems SR570 current preamplifier with a gain of 200 nA V^{-1}. After amplification, the signal at twice the actuation frequency is measured by an Agilent 35 670 A Dynamic Signal Analyzer at 50 Hz span. The received signal strength is -94 dBV_{rms}. The signal can be clearly received with a signal to noise ratio (SNR) of approximately 20 dB.

By sweeping the actuation signal frequency and observing the doubled frequency of reflected light intensity modulation, the mechanical frequency response of the MEMS optical cavity was measured. As shown in figure 11, the 3 dB bandwidth of the MEMS optical cavity was found to be nearly 40 kHz. The frequency response also shows the device to be underdamped with a resonance around 25 kHz. The estimated natural frequency from simulation was higher at 782 kHz, but was expected to be overdamped due to squeeze-film damping and spring effects. A defect in the release of the device in one corner, overetched springs, and the thickness tolerance of the SOI device and buried oxide layer may be contributing effects to the reduced bandwidth. Regardless, this bandwidth is more than sufficient for carrying data and communicating sensor measurements.

Coupling the MEMS optical cavity to optical fibers allows many possibilities for device interconnection. As shown in figure 12, we used two 0.75 mm diameter PMMA optical fibers to connect to the device. In a configuration similar to figure 1, one fiber sends in constant illumination, and one fiber captures the reflected light and carries it to the photodiode for measurement. Amplifying the photodiode signal at 1 μA V^{-1} we found a signal strength of -53 dBV_{rms} as measured by a Stanford Research Systems SR830 and a SNR of about 50 dB at a measurement span of 12.5 Hz as measured using an Agilent 35670A dynamic signal analyzer. Using two fibers we have demonstrated fiber-coupled communication using a MEMS optical cavity.

We can determine the energy required to send a bit of information by calculating the energy required to deflect the MEMS mirror. The energy required to deflect the mirror, $E_{actuation}$, depends on the stiffness of the springs, k, the distance deflected, d, the capacitance of the mirror, C, and the applied voltage V.

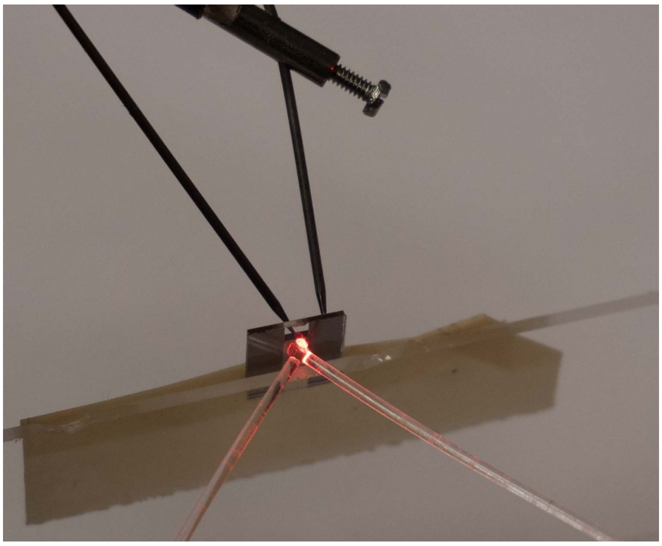

Figure 12. Device with optical fiber input and fiber output.

The capacitance of the MEMS mirror can be estimated as a parallel plate capacitor with an area the size of the mirror and springs themselves, approximately 200 μm by 250 μm. The distance between the capacitor plates is the distance between the mirror and the handle layer when actuated. The area of the die which is not the MEMS mirror can be neglected because in application, the die could be made considerably smaller, comparable to the mirror's size or electrically isolated from the surrounding area to reduce excess capacitance.

The energy stored in the springs is estimated from the spring constant and the deflection is estimated from optical profilometer data when the device is at rest at the applied actuation voltage. At the peak applied actuation voltage of 10 V the steady state deflection observed by the optical profilometer is about 6 nm.

The energy to actuate the mirror once can be calculated using equation (1)

$$E_{\text{actuation}} = \frac{1}{2}CV^2 + \frac{1}{2}kd^2. \tag{1}$$

Using equation (1), we estimate the actuation energy to be approximately 44 pJ per actuation. Further, because the deflection of the mirror is capacitive it may be possible to recover some of the expended energy when the mirror is restored to its original position, further reducing power consumption.

6. Conclusions

Communication using passive optical cavity transmitters compares favorably with other low power digital communication methods. One of the common communication methods used in distributed sensors is Bluetooth low energy (BLE). Low power BLE transmitters are reported to have energy per bit figures of around 3.5 nJ [19]. The method presented in this paper by comparison consumes almost 100× less energy per actuation. Further, this method also does not require an antenna which is bulky compared to our micro mirrors.

This paper successfully demonstrates electrostatically actuated MEMS optical cavities that passively communicate by modulating the intensity of reflected monochromatic light. We demonstrate that MEMS optical cavities can communicate with energies per actuation as low as 44 pJ using a mirror measuring only 250 μm by 200 μm at a bandwidth of ~40 kHz. We have also demonstrated that these MEMS optical cavities can be fiber-coupled using common PMMA optical fiber. We believe MEMS optical cavity transmitters can enable improved low power, compact, digital, distributed devices with onboard electrically connected sensors.

Data availability statement

All data that support the findings of this study are included within the article (and any supplementary files).

Funding

This material is based upon work supported by the National Science Foundation under Cooperative Agreement No. 1849213.

ORCID iDs

Jacob Schopp https://orcid.org/0009-0002-6910-6826
Shamus McNamara https://orcid.org/0000-0002-7342-4774

References

[1] Girão P S, Ramos P M P, Postolache O and Dias Pereira J M 2013 Tactile sensors for robotic applications *Measurement* **46** 1257–71
[2] Sundaram S, Kellnhofer P, Li Y, Zhu J-Y, Torralba A and Matusik W 2019 Learning the signatures of the human grasp using a scalable tactile glove *Nature* **569** 698–702
[3] Floris I, Adam J M, Calderón P A and Sales S 2021 Fiber optic shape sensors: a comprehensive review *Opt. Lasers Eng.* **139** 106508
[4] Ukil A, Braendle H and Krippner P 2012 Distributed temperature sensing: review of technology and applications *IEEE Sens. J.* **12** 885–92
[5] Bado M F and Casas J R 2021 A review of recent distributed optical fiber sensors applications for civil engineering structural health monitoring *Sensors* **21** 1818
[6] Wu T, Liu G, Fu S and Xing F 2020 Recent progress of fiber-optic sensors for the structural health monitoring of civil infrastructure *Sensors* **20** 4517
[7] Kandris D, Nakas C, Vomvas D and Koulouras G 2020 Applications of wireless sensor networks: an up-to-date survey *Appl. Syst. Innov.* **3** 14
[8] Shaikh F K and Zeadally S 2016 Energy harvesting in wireless sensor networks: a comprehensive review *Renew. Sustain. Energy Rev.* **55** 1041–54
[9] Ijemaru G K, Ang K L-M and Seng J K P 2022 Wireless power transfer and energy harvesting in distributed sensor networks: survey, opportunities, and challenges *Int. J. Distrib. Sens. Netw.* **18** 15501477211067740
[10] Masoudi A and Newson T P 2016 Contributed review: distributed optical fibre dynamic strain sensing *Rev. Sci. Instrum.* **87** 011501

[11] Pospíšilová M, Kuncová G and Trögl J 2015 Fiber-optic chemical sensors and fiber-optic bio-sensors *Sensors* **15** 25208–59
[12] Katrenova Z, Alisherov S, Abdol T and Molardi C 2024 Status and future development of distributed optical fiber sensors for biomedical applications *Sens. Bio-sens. Res.* **43** 100616
[13] Jasjot K S, Neena G and Divya D 2020 Fiber Bragg grating sensors for monitoring of physical parameters: a comprehensive review *Opt. Eng.* **59** 060901
[14] Shadab A, Raghuwanshi S K and Kumar S 2022 Advances in micro-fabricated fiber Bragg grating for detection of physical, chemical, and biological parameters—a review *IEEE Sens. J.* **22** 15650–60
[15] Lu P, Lalam N, Badar M, Liu B, Chorpening B T, Buric M P and Ohodnicki P R 2019 Distributed optical fiber sensing: review and perspective *Appl. Phys. Rev.* **6** 041302
[16] Bao X and Wang Y 2021 Recent advancements in Rayleigh scattering-based distributed fiber sensors *Adv. Devices Instrum.* **2021** 8696571
[17] Froemel J, Baum M, Wiemer M, Roscher F, Haubold M, Jia C and Gessner T 2011 Investigations of thermocompression bonding with thin metal layers *2011 16th Int. Solid-State Sensors, Actuators and Microsystems Conf.: IEEE* pp 990–3
[18] Malik N, Schjølberg-Henriksen K, Poppe E, Taklo M M V and Finstad T G 2014 Al–Al thermocompression bonding for wafer-level MEMS sealing *Sens. Actuators* A **211** 115–20
[19] Abdelatty O, Bishop H, Shi Y, Chen X, Alghaihab A, Calhoun B H and Wentzloff D D 2019 A low power Bluetooth low-energy transmitter with a 10.5nJ startup-energy crystal oscillator *ESSCIRC 2019—IEEE 45th European Solid State Circuits Conf. (ESSCIRC)* pp 377–80